Supporting Information

Application of *in-situ* ATR-IR Spectroscopy in Bisphenol F Synthetic Process: Optimization, Mechanistic and Kinetics Study

Yun Zhao*[ab], XinKai Zhang[a], Yanxia Chen[a], Pingyi Zhang, Haifang Mao*[ab]

[a]Shanghai Institute of Technology, 100 Haiquan Road, Shanghai, China.

[b]Shanghai Research Institute of Fragrance & Flavor Industry, 480 Nanning Road, Shanghai, China.

1 Experimental sections

ESI 1: HPLC analysis for Bisphenol F

All the experimental conditions for HPLC tests were the same during the whole work.

Chromatographic column: C18 column (4.6 mm×250 mm, 5 μm)

Column temperature: 25 ℃

Detection wavelength: 274 nm

Injection volume:10 μL

Flow rate: 1.0 mL/min

Mobile phase:

A---Acetonitrile (HPLC);

B--- distilled water;

Gradient elution method was adopted (see the table below):

Time /min	A volume/%	B volume/%
0	30	70
8	50	50
11	55	45
13	30	70
14	30	70
15	30	70
16	55	45
20	55	45
20	30	70
30	30	70

Quantification of BPF isomers were carried out with external standard curve method.

$$\text{BPF total yield (\%)}=\frac{n_{4,4'-BPF}+n_{2,4'-BPF}+n_{2,2'-BPF}}{n_{BPF,theoretical}}\times 100\%$$

$$\text{4,4'-BPF selectivity (\%)}=\frac{n_{4,4'-BPF}}{n_{4,4'-BPF}+n_{2,4'-BPF}+n_{2,2'-BPF}}\times 100\%$$

4,4'-BPF yield (%)=BPF total yield×4,4'-BPF selectivity

where,

$n_{4,4'\text{-BPF}}$, $n_{2,4'\text{-BPF}}$ and $n_{2,2'\text{-BPF}}$ were quantified with external standard curve;

$n_{\text{BPF, theoretical}}$ is the calculated based on the input amount of formaldehyde, $n_{BPF,theoretical} = n_{formaldehyde} \times 200.24$(molecular weight of BPF).

ESI 2: Exploration of reaction sequence

Step 1: Reaction of phenol with phosphoric acid

20.01 g phenol was added into a 250 mL four-mouth flask and the temperature was raised to 52 ºC. Then inserted the ATR-IR probe into the reaction bottle, 25.36 g phosphoric acid was dropped into the bottle slowly, then monitoring the IR spectra. Peak located at 695 cm^{-1} ($\delta_{C\text{-}H}$, phenol) and 863 cm^{-1} ($\nu_{P\text{-}(OH)3}$, phosphoric acid) were selected as the characteristic peaks. Monitoring the concentration variation of phenol while observing whether there were any new peaks which neither belong to phenol nor to phosphoric acid appeared.

Step 2: Reaction of formaldehyde with phosphoric acid

45.8 g 37% formaldehyde was added into a 250 mL four-mouth flask and the temperature was raised to 52 ºC. Then inserted the ATR-IR probe into the reaction bottle, 25.36 g phosphoric acid was dropped into the bottle slowly, then monitoring the IR spectra. Peak located at 1070 cm^{-1} ($\nu_{O\text{-}C\text{-}O}$, formaldehyde) was selected as the characteristic peaks. Monitoring the concentration variation of formaldehyde while observing whether there were any new peaks which neither belong to formaldehyde nor to phosphoric acid appeared. *In-situ* Raman monitoring was carried out in a similar way, with a Raman probe alternative to ATR-IR probe.

ESI 3: Establishment of the mid-infrared quantification model for 4,4'-bisphenol F to guide the optimization of experimental conditions

The typical process includes the following steps:

① Find out the characteristic peaks for 4,4'-BPF by measuring the IR spectrum of the pure substance. Herein, since there was no interference from 2,2'-BPF and 2,4'-BPF, the relatively more sensitive stretching vibration of C=C bond located at 1515 cm^{-1} was therefore selected as the characteristic peak for 4,4'-BPF.

② Establish the external quantification curve for 4,4'-BPF by HPLC analysis;

③ Link the IR characteristic peak intensity of 4,4'-BPF with different concentration to the corresponding quantification result from HPLC external curve and establish the *in-situ* mid-infrared quantification model with the help of ICQuant Model (Mettler software); Typically, the abscissa is the actual value measured by HPLC, and the ordinate is the predicted value by IR quantification model. In this work, the concentration range for 4,4'-BPF was 4.0~100 mg/mL.

④ Adjusted the key experimental parameters (P/F ratio, reaction temperature, stirring

speed, catalyst dosage, etc) and used the established IR quantification model to monitor the concentration of 4,4'-BPF under different experimental conditions. Herein, the highest concentration of 4,4'-BPF indicated an optimized experimental condition.

ESI 4: Establishment of the mid-infrared quantification model for phenol and formaldehyde

The typical process includes the following steps:

① Find out the characteristic peaks for phenol and formaldehyde by measuring the IR spectrum of the pure substance;

② Establish the external quantification curve for both substances by HPLC analysis;

③ Link the IR characteristic peak intensity of phenol (1478 cm^{-1}, δ_{O-H}) and formaldehyde (1029 cm^{-1}, ν_{C-O}) with different concentration to the corresponding quantification result from HPLC external curve and establish the *in-situ* mid-infrared quantification model with the help of ICQuant Model (Mettler software); Typically, the abscissa is the actual value measured by HPLC, and the ordinate is the predicted value by IR quantification model. In this work, the concentration range for phenol was 10~90 mg/mL while the concentration range for formaldehyde was 5.0~ 45 mg/mL.

2 Supporting Figures and Tables

Fig. S1 Original mid-infrared spectra for phenol, phosphoric acid and formaldehyde.

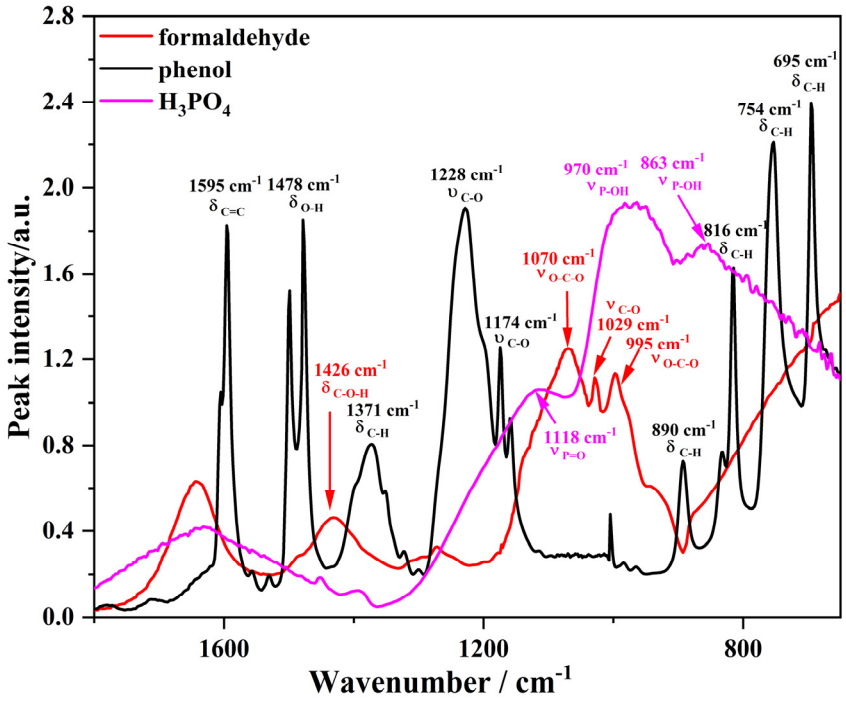

Fig. S1 Original mid-infrared spectra for phenol (black), formaldehyde (red) and phosphoric acid (pink).

Table S1 Characteristic peaks attributions for phenol, phosphoric acid and formaldehyde.

Table S1 Characteristic peaks attributions.

Substances	Absorption peak position /cm^{-1}	Peak attribution	Reference
phenol	695	C-H bendings of the benzene ring	1
	754		
	816		
	890		
	1174	C-O stretchings of benzene ring	
	1228		
	1371	C-H bendings	
	1478	O-H deformation of phenols	2
	1595	Aromatic C=C bending	3
formaldehyde	995	$\nu_{O\text{-}C\text{-}O}$	4
	1029	$\nu_{C\text{-}O\text{-}C}$ in oligomers	
	1070	$\nu_{O\text{-}C\text{-}O}$	
	1426	$\delta_{C\text{-}O\text{-}H}$ in plane	
H_3PO_4	863	$\nu_{P(OH)3}$	5, 6
	970	$\nu_{P\text{-}(OH)3}$	
	1118	$\nu_{P=O}$	

Fig. S2 *In-situ* trend monitoring of characteristic mid-infrared peaks of phenol and phosphoric acid when adding phosphoric acid to phenol without the presence of formaldehyde.

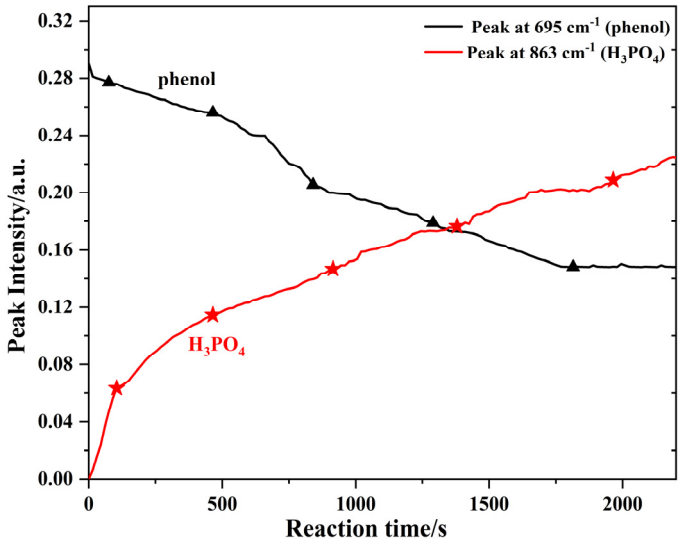

Fig. S2 *In-situ* trend monitoring of characteristic mid-infrared peaks of phenol (black) and

phosphoric acid (red) when adding phosphoric acid to phenol without formaldehyde (second derivative diagram).

The initial concentration of phenol was 1.071 g/mL, corresponding to a peak height of 0.28. After the addition of 25.36 g phosphoric acid (85%), the peak height decreased to 0.148. From $\triangle h$=0.132, we could infer that $\triangle c_{phenol}$ =0.504 g/mL. Through the calculation of phosphoric acid volume, we could calculate that the concentration of phenol after phosphoric acid addition was 0.567 g/mL, that means the concentration variation of phenol was 1.071 g/mL - 0.567 g/mL=0.504 g/mL, accorded well with the peak height decrease. Therefore, the decrease in phenol characteristic peak was not caused by the interaction between phenol and catalyst, but due to the volume dilution after catalyst addition.

Fig. S3 *In-situ* Raman spectra of formaldehyde and phosphoric acid reaction

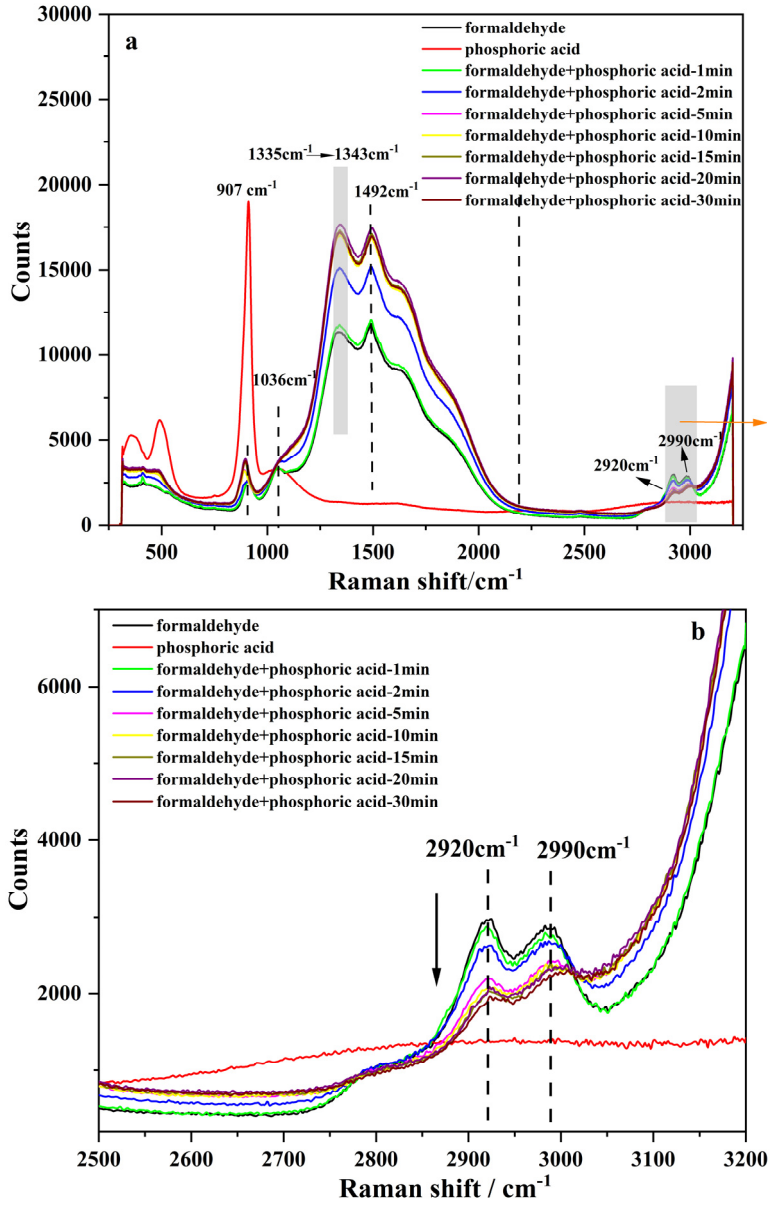

Fig. S3 *In-situ* Raman spectra of formaldehyde and phosphoric acid reaction, (b) is the enlarge of grey part in (a).

Seen from Fig. S3a, formaldehyde exhibited two strong characteristic peaks located at 1335 cm^{-1} and 1492 cm^{-1}, corresponding to τ(HCH) and δ(HCH) vibration[7]. The other three characteristic peaks located at 907 cm^{-1}, 2920 cm^{-1} and 2990 cm^{-1} were attributed to *v*s(OCO)[8], *v*s(HCH) and *v*a(HCH)[7], respectively, indicating that formaldehyde was in a hydrated form $CH_2(OH)_2$. With the addition of catalyst H_3PO_4, peaks located at 2920 cm^{-1} and 2990 cm^{-1} gradually decreased (Fig. S3b), accompanied by the disappearance of catalyst characteristic peak (1036 cm^{-1}, $\nu_{P\text{-}O(H)}$)[6]. Meanwhile, peaks at 1335 cm^{-1} gradually shifted to 1343 cm^{-1} and the intensity of it exhibited an obvious increase, as well as that of peak 1492 cm^{-1}, indicating that the chemical environment of HCH bond in hydrated formaldehyde experienced a change in the presence of acid. Therefore, we attributed these two strong peaks to the activated product $^{+}CH_2OH$ caused by the reaction between catalyst and formaldehyde.

Fig. S4 Original IR spectra for two intermediates and three bisphenol F isomers

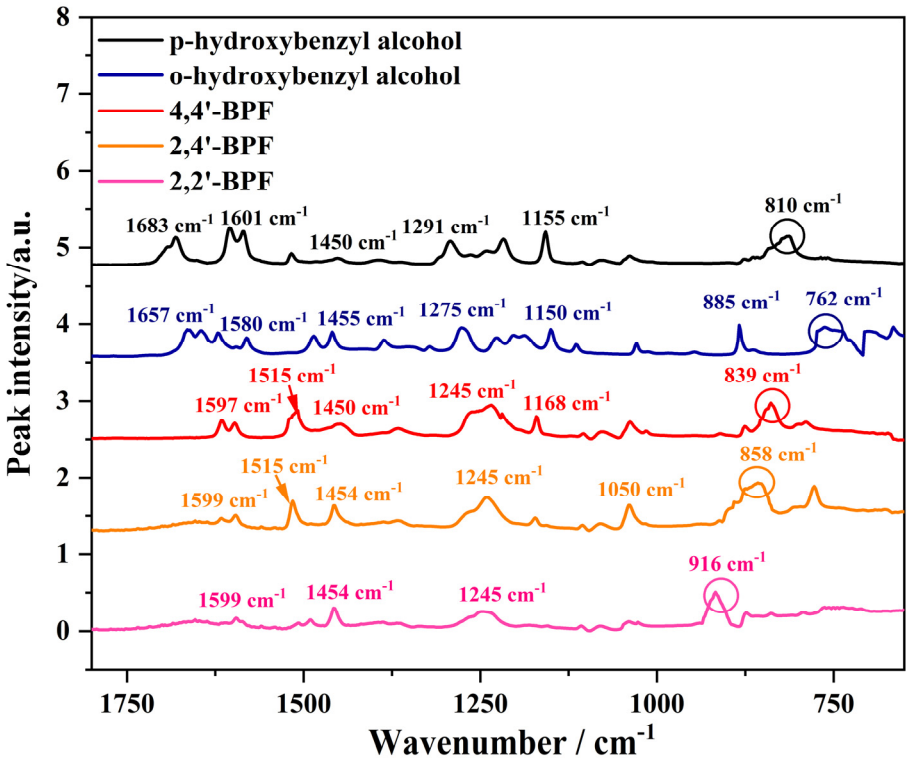

Fig. S4 Original mid-infrared spectra of two hydroxybenzyl alcohol intermediates and three BPF isomers.

Table 2 Characteristic peaks attributions for phenol, phosphoric acid and formaldehyde.

Table S2 Characteristic peaks attributions.

Absorption peak position /cm^{-1}	Peak attribution	Reference
762~885	C–H bendings of the benzene ring	1
916	$\upsilon_{C\text{-}C}+\delta_{C\text{-}H}$	9
1050~1245	$\nu_{C\text{-}O}$ of benzene ring	1
1250~1300	aromatic ring	2
1450~1455	$\delta_{C\text{-}H}$	1
1500~1700	aromatic C=C bending	3

Fig. S5 HPLC profiles monitoring intermediates generation

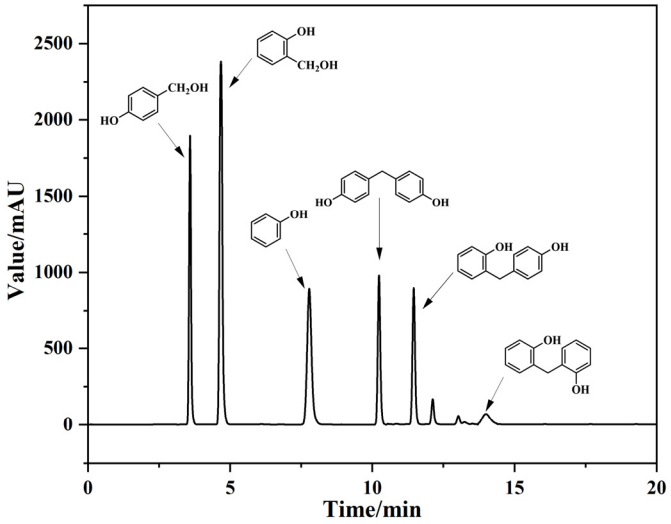

Fig. S5 HPLC profiles monitoring intermediates generation

Fig. S6 HPLC profiles of products generation

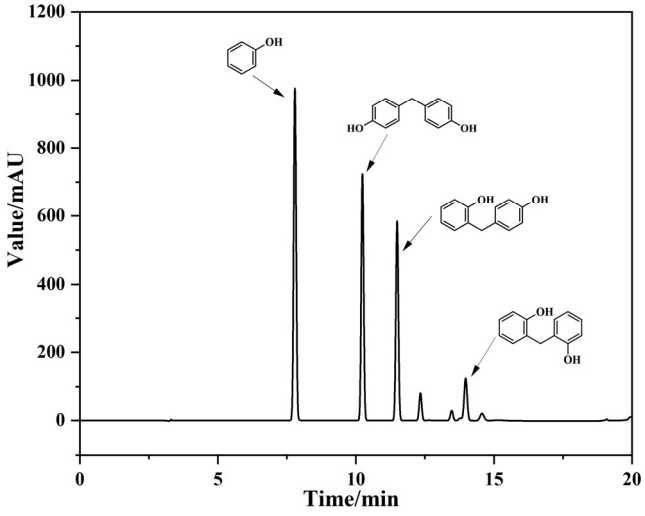

Fig. S6 HPLC profiles of products generation

Fig. S7 FT-IR spectra for 4,4'-BPF with different concentration

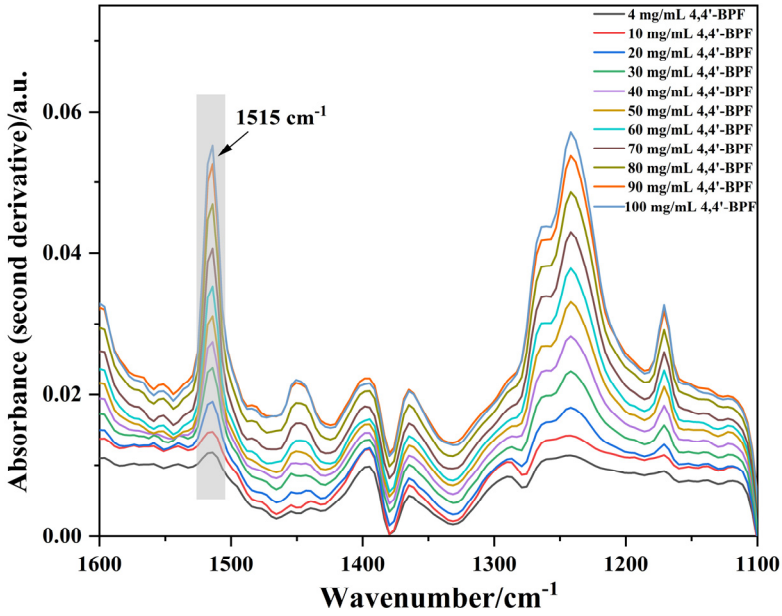

Fig. S7 Mid-infrared spectra of 4,4'-BPF with different concentration (second derivative diagram).

Fig. S8 FT-IR spectra and FT-IR quantification model for phenol (a,b) and formaldehyde (c,d)

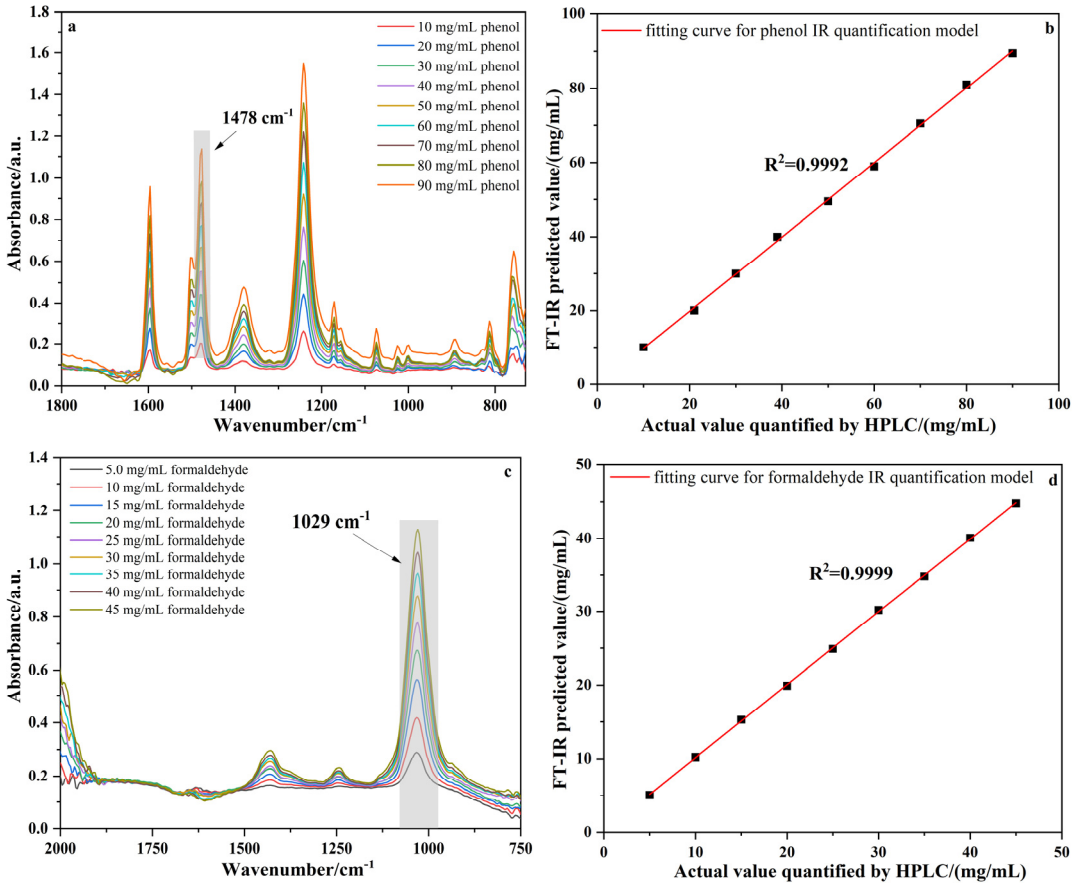

Fig. S8 Mid-infrared spectra of phenol (a) and formaldehyde (c) solution with different concentration; Mid-infrared quantification model for phenol (b) and formaldehyde (d).

Fig. S9~S12 Kinetic curves and fitting curves under different temperatures (40 ℃, 60 ℃, 70 ℃, 80 ℃)

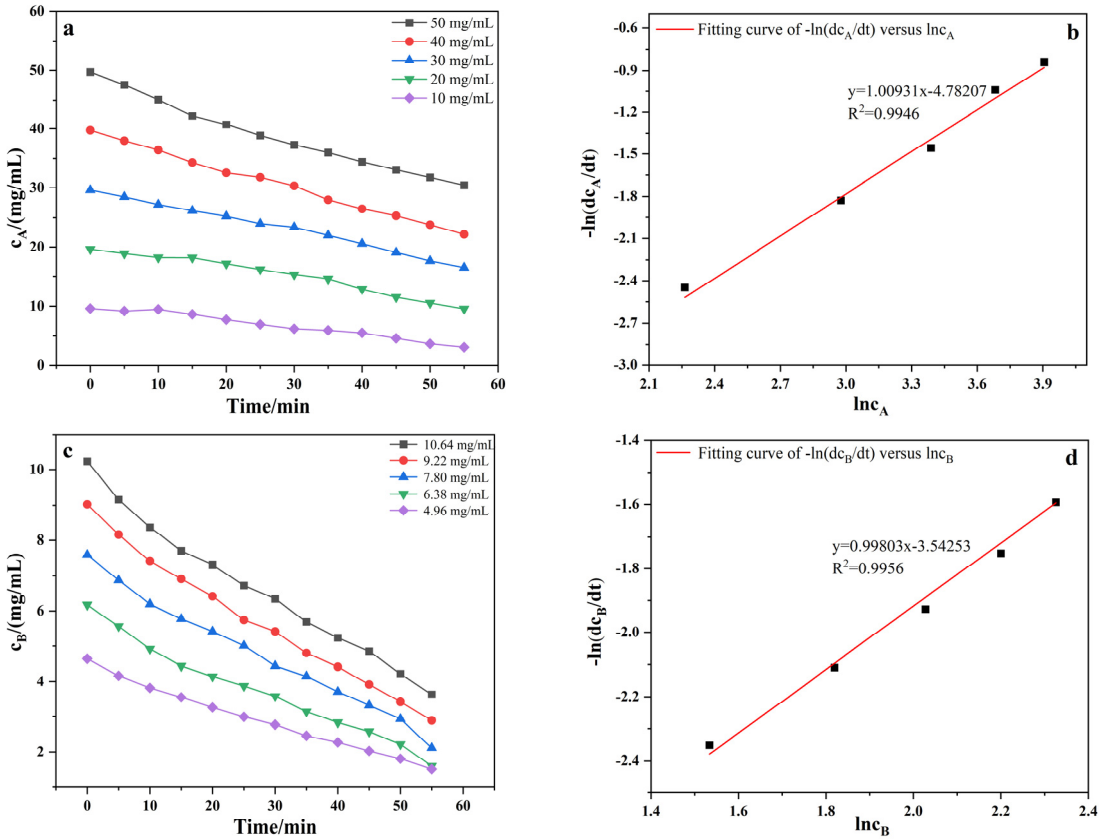

Fig. S9 (a) The influence of initial concentration of phenol on the reaction rate at 40 ℃; (b) $\ln\left(\frac{dc_A}{dt}\right)$-$lnc_{A,0}$ fitted curve at 40 ℃; (c) formaldehyde concentration versus reaction time under 40 ℃; (d) $-\ln\left(\frac{dc_B}{dt}\right)$-$lnc_{B,0}$ fitted curve at 40 ℃

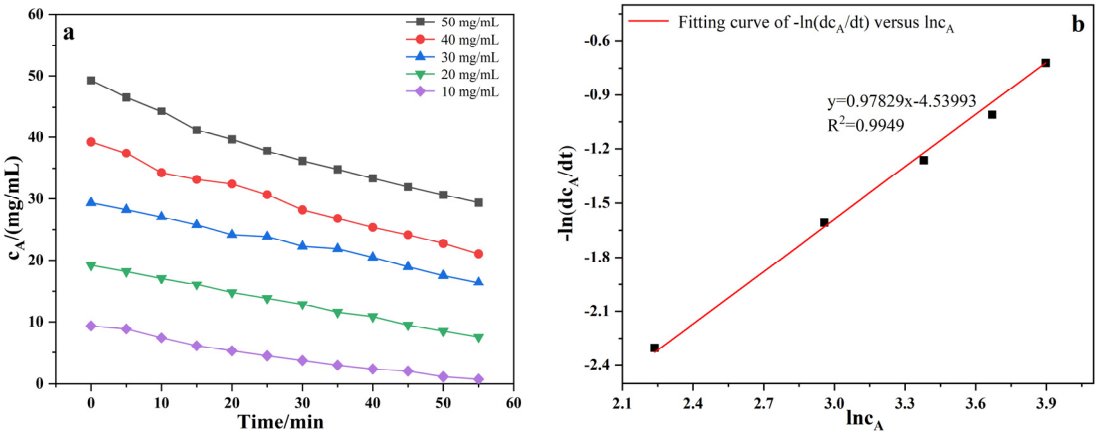

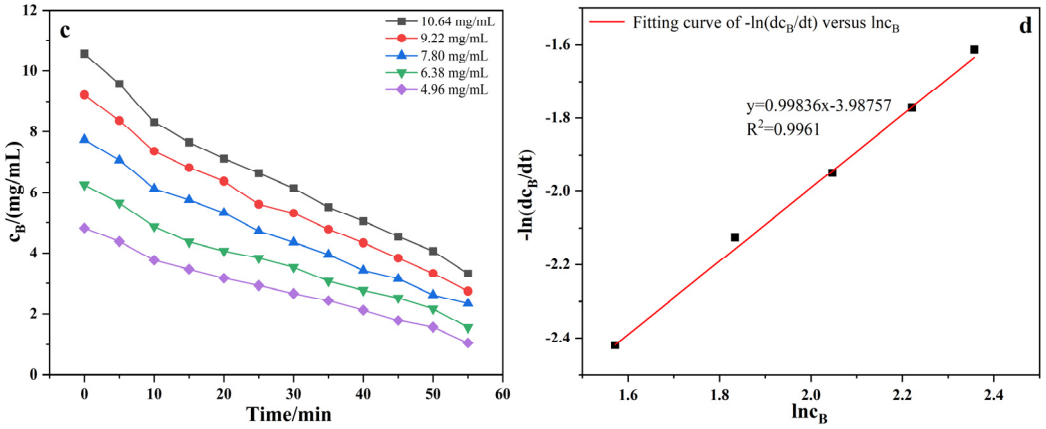

Fig. S10 (a) The influence of initial concentration of phenol on the reaction rate at 60 ℃; (b) $\ln\left(\frac{dc_A}{dt}\right)$-$lnc_{A,0}$ fitted curve at 60 ℃; (c) formaldehyde concentration versus reaction time under 60 ℃; (d) $-\ln\left(\frac{dc_B}{dt}\right)$-$lnc_{B,0}$ fitted curve at 60 ℃

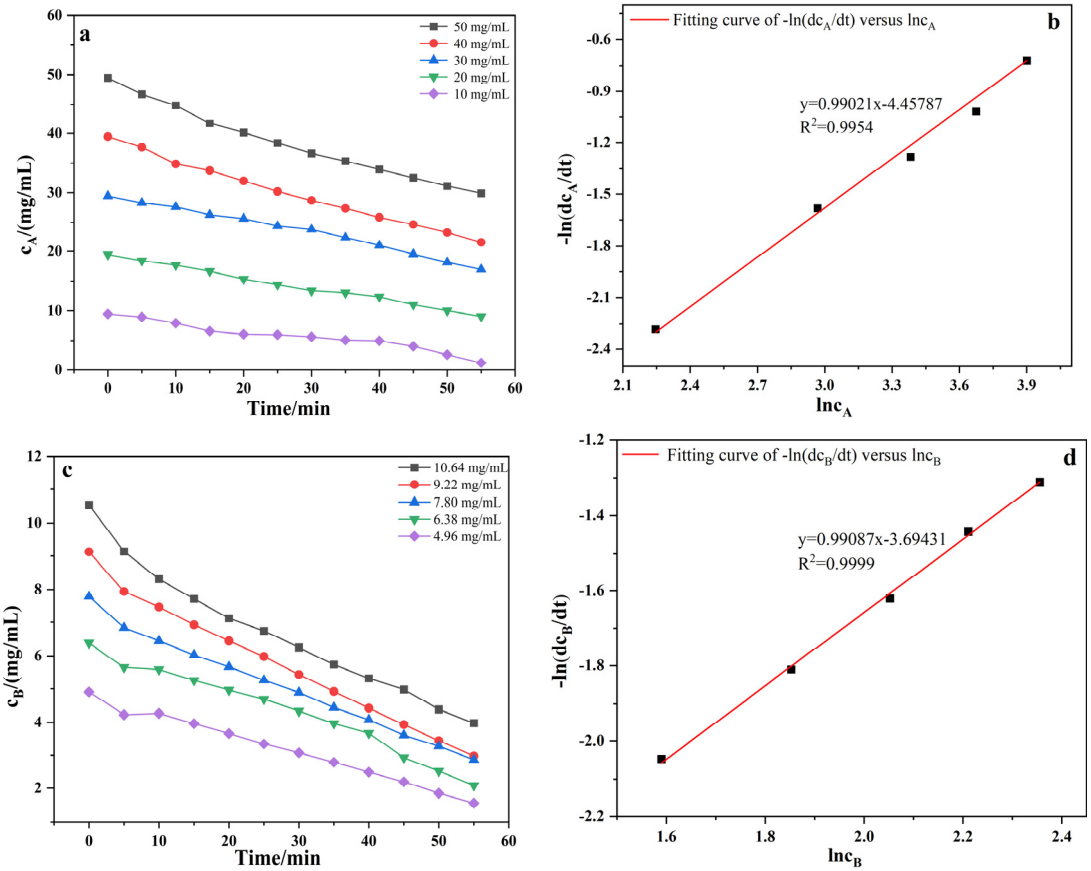

Fig. S11 (a) The influence of initial concentration of phenol on the reaction rate at 70 ℃; (b) $\ln\left(\frac{dc_A}{dt}\right)$-$lnc_{A,0}$ fitted curve at 70 ℃; (c) formaldehyde concentration versus reaction time under 70 ℃; (d) $-\ln\left(\frac{dc_B}{dt}\right)$-$lnc_{B,0}$ fitted curve at 70 ℃

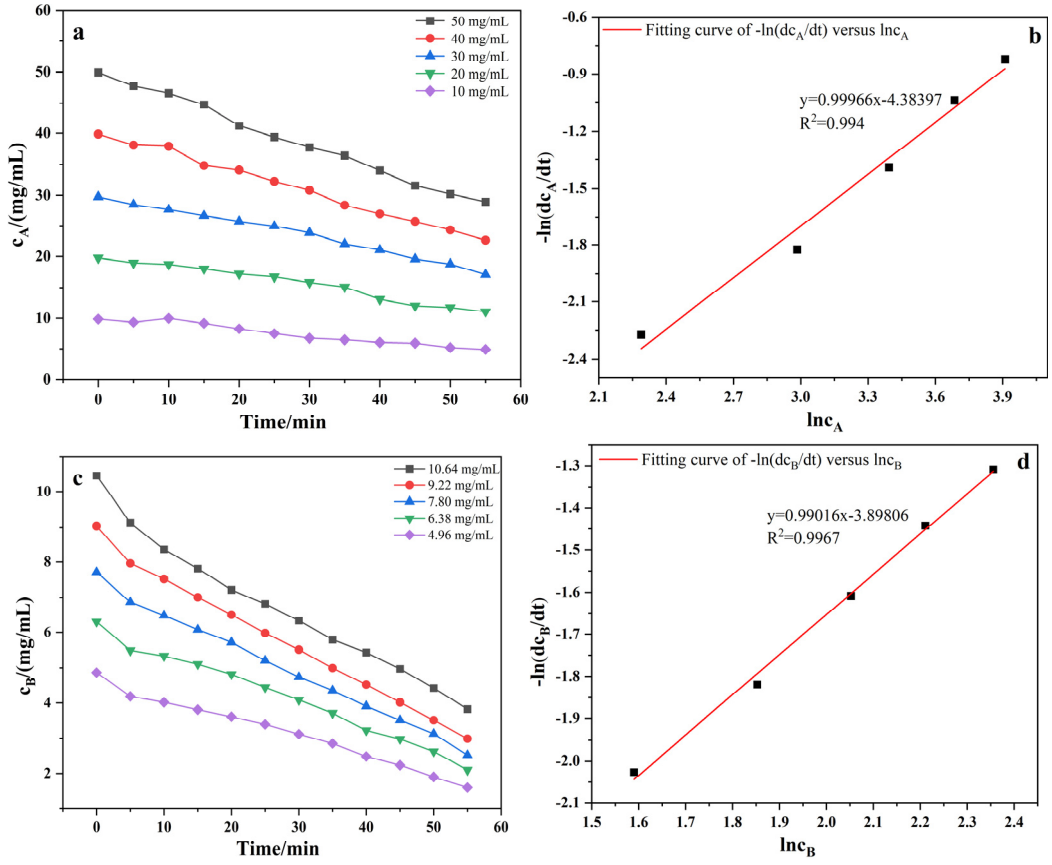

Fig. S12 (a) The influence of initial concentration of phenol on the reaction rate at 80 ℃; (b) $\ln\left(\frac{dc_A}{dt}\right)$-$lnc_{A,0}$ fitted curve at 80 ℃; (c) formaldehyde concentration versus reaction time under 80 ℃; (d) $-\ln\left(\frac{dc_B}{dt}\right)$-$lnc_{B,0}$ fitted curve at 80 ℃

1. Amiraslanova, M. N.; Alieva, A. P.; Akhmedbekova, S. F.; Ibragimova, M. D.; Mamedzade, F. A.; Rustamov, R. A.; Alieva, S. R.; Dadasheva, N. R.; Isaeva, P. E., Using IR Spectroscopy to Study Structures of Benzylamine Phenol-Formaldehyde Oligomers. *Journal of Structural Chemistry* **2019,** *60* (7), 1037-1042.
2. Moreno-Ley, C. M.; Hernández-Martínez, D. M.; Osorio-Revilla, G.; Tapia-Ochoategui, A. P.; Dávila-Ortiz, G.; Gallardo-Velázquez, T., Prediction of coumarin and ethyl vanillin in pure vanilla extracts using MID-FTIR spectroscopy and chemometrics. *Talanta* **2019,** *197*, 264-269.
3. Guerrero-Pérez, M. O.; Patience, G. S., Experimental methods in chemical engineering: Fourier transform infrared spectroscopy—FTIR. *The Canadian Journal of Chemical Engineering* **2020,** *98* (1), 25-33.
4. Gaca-Zając, K. Z.; Smith, B. R.; Nordon, A.; Fletcher, A. J.; Johnston, K.; Sefcik, J., Investigation of IR and Raman spectra of species present in formaldehyde-water-methanol systems. *Vibrational Spectroscopy* **2018,** *97*, 44-54.
5. Rudolph, W. W., Raman-and infrared-spectroscopic investigations of dilute aqueous phosphoric acid solutions. *Dalton Transactions* **2010,** *39* (40), 9642-9653.
6. Colthup, N., *Introduction to infrared and Raman spectroscopy*. Elsevier: 2012.

7. Lebrun, N.; Dhamelincourt, P.; Focsa, C.; Chazallon, B.; Destombes, J.; Prevost, D., Raman analysis of formaldehyde aqueous solutions as a function of concentration. *Journal of Raman Spectroscopy* **2003,** *34* (6), 459-464.
8. Matsuura, H.; Yamamoto, M.; Murata, H., Raman spectra and normal vibrations of methylene glycol and its perdeuterated analogue. *Spectrochimica Acta Part A: Molecular Spectroscopy* **1980,** *36* (3), 321-327.
9. Balachandran, V.; Murugan, M.; Karpagam, V.; Karnan, M.; Ilango, G., Conformational stability, spectroscopic (FT-IR & FT-Raman), HOMO-LUMO, NBO and thermodynamic function of 4-(trifloromethoxy) phenol. *Spectrochim Acta A Mol Biomol Spectrosc* **2014,** *130*, 367-75.